HHS Public Access

Author manuscript

Int J Pharm. Author manuscript; available in PMC 2015 November 12.

Published in final edited form as:

Int J Pharm. 2014 May 15; 466(0): 1–7. doi:10.1016/j.ijpharm.2014.03.016.

Dual-responsive polymer-coated iron oxide nanoparticles for drug delivery and imaging applications

Varsha Sundaresan[a,b], **Jyothi U. Menon**[a,b], **Maham Rahimi**[c], **Kytai T. Nguyen**[a,b], and **Aniket S. Wadajkar**[a,b,*]

[a]Department of Bioengineering, The University of Texas at Arlington, Arlington, TX 76019, United States

[b]Joint Biomedical Engineering Program between The University of Texas at Arlington and The University of Texas Southwestern Medical Center, Dallas, TX 75390, United States

[c]Department of Vascular Surgery, University of Cincinnati, OH 45267, United States

Abstract

We reported the synthesis and characterization of dual-responsive poly(*N*-isopropylacrylamide-acrylamide-chitosan) (PAC)-coated magnetic nanoparticles (MNPs) for controlled and targeted drug delivery and imaging applications. The PAC-MNPs size was about 150 nm with 70% iron mass content and excellent superparamagnetic properties. PAC-MNPs loaded with anti-cancer drug doxorubicin showed dual-responsive drug release characteristics with the maximum release of drugs at 40 °C (~78%) than at 37 °C (~33%) and at pH of 6 (~55%) than at pH of 7.4 (~28%) after 21 days. Further, the conjugation of prostate cancer-specific R11 peptides increased the uptake of PAC-MNPs by prostate cancer PC3 cells. The dose-dependent cellular uptake of the nanoparticles was also significantly increased with the presence of 1.3 T magnetic field. The nanoparticles demonstrated cytocompatibility up to concentrations of 500 μg/ ml when incubated over a period of 24 h with human dermal fibroblasts and normal prostate epithelial cells. Finally, pharmacokinetic studies indicated that doxorubicin-loaded PAC-MNPs caused significant prostate cancer cell death at 40 °C than at 37 °C, thereby confirming the temperature-dependent drug release kinetics and *in vitro* therapeutic efficacy. Future evaluation of *in vivo* therapeutic efficacy of targeted image-guided cancer therapy using R11-PAC-MNPs will reinforce a significant impact of the multifunctional PAC-MNPs on the future drug delivery systems.

Keywords

Poly(*N*-isopropylacrylamide); Chitosan; Iron oxide magnetic nanoparticles; Prostate cancer; Dual-responsiveness

*Corresponding author at: The University of Texas at Arlington, Bioengineering, 500 UTA Blvd, ERB 282 Arlington, TX 76019, United States. Tel.: +1 817 805 2448; fax: +1 817 272 2251. aniketwadajkar@yahoo.com, aniket.wadajkar@mavs.uta.edu (A. S. Wadajkar).

1. Introduction

Temperature-sensitive polymers such as poly(*N*-isopropylacrylamide) (PNIPAAm) have been widely used in drug delivery systems to release drugs in response to the changes in surrounding temperature (Schmaljohann, 2006). Copolymerization of PNIPAAm with hydrophilic acrylamide (AAm)has shown success inincreasing the lower critical solution temperature (LCST) of PNIPAAm from 32 °C to the temperatures above physiological temperature, which is more suitable for *in vivo* controlled drug release (Rahimi et al., 2010). However, the non-biodegradable nature of PNIPAAm limits its widespread *in vivo* use due to the possibility of accumulation, toxicity and inflammatory responses (Cui et al., 2011).

To overcome the non-biodegradability limitation, PNIPAAm has been copolymerized with a variety of natural polymers employing their properties of biodegradability (Dash et al., 2011). For example, PNIPAAm hydrogels have been grafted with natural polymers such as chitosan, collagen, and gelatin to form a degradable gel (Curcio et al., 2010; Fitzpatrick et al., 2010). Biocompatible chitosan is a cationic polysaccharide that enzymatically degrades *in vivo* at physiological conditions and has been extensively studied for biomedical applications (Dash et al., 2011; Yomota et al., 1990). Copolymerization of PNIPAAm with chitosan thus makes it degradable to have PNIPAAm in smaller fragments, such as dimers and trimers. Such small length PNIPAAm can be easily removed out of the body by renal clearance (Patenaude and Hoare, 2012). Chitosan also displays pH-sensitivity due to protonation–deprotonation of a large number of amino groups present (Chuang et al., 2010). Further, incorporation of super-paramagnetic iron oxide magnetic nanoparticles (MNPs) adds further functionalities to the design, such as non-invasive image-guided magnetic targeting, contrast agents for magnetic resonance imaging (MRI), hyperthermia of solid tumors, providing heat and stimulating drug release from thermo-sensitive polymer (Rosen et al., 2012; Sun et al., 2008). Besides magnetic targeting, active targeting of nanoparticles to the tumor site has also been effective in cancer treatment due to increased specificity and bioavailability of particles at the target site (Danhier et al., 2010). A variety of targeting ligands such as antibodies, aptamers, folic acid, and RGD peptides have shown promise in prostate cancer targeting (Sethuraman and Bae, 2007). Recently, the cell-penetrating R11 peptides have been proven to have the ability to bind to prostate cells at specific sites such as the laminin receptor site and also have the potential to be useful in prostate cancer detection (Zhou et al., 2012).

Encompassing the advantages of PNIPAAm, AAm, chitosan, MNPs, and R11 peptides, our aim was to synthesize and characterize R11-conjugated, drug-loaded PNIPAAm-AAm-chitosan (PAC)-coated MNPs (PAC-MNPs) as a potential drug delivery and imaging system for prostate cancer management. PNIPAAm-chitosan nanogels have previously been synthesized without AAm, MNPs, and targeting ligands for drug delivery and tissue engineering applications (Chuang et al., 2009; Li et al., 2009). In our design, the differences with these studies are that the R11 peptides and magnetic guidance can ensure that the particles reach the site of action. Furthermore, an external magnetic field can be used to heat up the MNPs, leading to hyperthermia and temperature-responsive drug release from polymer shell. In addition, the pH-responsiveness provides an added advantage of delivering the drugs only to the tumor, owing to its extracellular acidic pH (Min et al., 2010b).

Employing our PAC-MNPs in cancer therapy would facilitate a biocompatible, degradable, tumor-targeted, dual-responsive drug release and magnetic hyperthermia/imaging system. The dual-targeting (magnetic targeting and receptor-mediated targeting) capability of particles combined with dual-responsive (pH and temperature) drug release would provide a highly specific and efficient system for cancer treatment.

2. Experimental

2.1. Materials

All the materials were purchased from Sigma–Aldrich (St. Louis, MO), if not mentioned. Ferric oxide magnetic nanoparticles (MNPs, Meliorum Technologies, Rochester, NY), doxorubicin (Dox, Tocris Bioscience, Ellisville, MO), and R11 peptides (Anaspec, Fremont, CA) were purchased and used without further purification. Roswell Park Memorial Institute medium (RPMI), neonatal calf serum (NCS), penicillin–streptomycin, and Trypsin were purchased from Invitrogen, Carlsbad, CA. Clonetics® Prostate Endothelial Basal Medium (PrEBM™) and SingleQuots® Kit Supplements & Growth Factors (PrEGM™) were purchased from Lonza, Walkersville, MD. Whereas, human dermal fibroblasts (HDFs), normal prostate epithelial cells (PZ-HPV-7), and prostate cancer cells (PC3) were purchased from ATCC, Manassas, VA.

2.2. Synthesis of PAC nanoparticles, PAC-MNPs, and R11-conjugated PAC-MNPs

PAC nanoparticles were prepared by free radical graft copolymerization. Briefly, 0.25 g chitosan was added to 5% acetic acid solution. After complete dissolution, 0.886 g *N*-isopropylacrylamide (NIPAAm), 0.1137 g AAm and 0.01 g *N*,*N*-methylenebisacrylamide (BIS) were added and the reaction was heated to 80 °C. Polymerization was initiated by adding 1.44 ml tert-butyl hydroperoxide (TBHP); the reaction was purged with N_2 and stirred for 3 h. As-prepared PAC nanoparticles were purified by dialyzing against deionized (DI) water overnight using 100 kDa cut-off dialysis membranes (Spectrum Laboratories Inc., Rancho Dominguez, CA).

For PAC-MNPs, silane-functionalized MNPs were prepared as reported previously (Wadajkar et al., 2012b). Briefly, 0.74 g MNPs were dispersed in 100 ml of 99% ethanol solution. Then, 3 ml acetic acid was added and sonication was continued for another 10 min. The reaction was transferred to a magnetic stirring plate; 0.49 ml vinyltrimethoxysilane (VTMS) was added and stirred for 24 h. The silane-functionalized MNPs were collected using a magnet and washed several times with 99% ethanol solution. These particles were then used as a template to form core-shell PAC-MNPs following the same protocol as PAC nanoparticles, as described earlier. Briefly, 0.028 g silane-functionalized MNPs were suspended in 5% acetic acid solution by sonication, after which chitosan, NIPAAm, AAm, BIS, and TBHP were added. The reaction was carried in the same way as mentioned above, and PAC-MNPs were washed and collected using a magnet.

Further, R11 peptides specific to prostate cells were conjugated to PAC-MNPs using carbodiimide chemistry. Briefly, 1.75 μl R11 peptide solution (10 μM) was added to 5 mg *N*-(3-dimethylaminopropyl)-*N*′-ethylcarbodiimidehydrochloride (EDC) in 0.5 ml 2-(*N*-morpholino) ethanesulfonic acid (MES) buffer. After 30 min of shaking, 5 mg *N*-

Hydroxysuccinimide (NHS) was added and left for another 30 min for shaking. Separately, 1 mg PAC-MNPs were suspended in 0.5 ml MES buffer by sonication; added to above solution and incubated for 12 h at room temperature on a shaker. The R11-conjugated PAC-MNPs (R11-PAC-MNPs) were washed several times with DI water and collected using a magnet.

2.3. Characterization

Scanning electron microscope (SEM, S-3000N, Hitachi, Pleasanton, CA) and transmission electron microscope (TEM, FEI Technai G2 Spirit BioTWIN, Hillsboro, OR) were used to analyze the particle size, shape and morphology. Dynamic light scattering (DLS, ZetaPals, Brookhaven Instruments, Holtsville, NY) was used to measure the particle size and polydispersity index. Fourier transform infrared spectroscopy (FTIR, Nicolet 6700, Thermo Scientific, Madison, WI) was performed to confirm the presence of the characteristic peaks of the bonds in the PAC. The LCST of the particles was evaluated by spectrophotometry (Smartspec™ plus, Bio-Rad Laboratories, Philadelphia, PA). Briefly, absorbance of the particle solution at 500 nm was measured from 25 °C to 50 °C with an increment of 1 °C. The graph of temperature *vs*. transmittance was plotted and the temperature at 50% transmittance was noted as the LCST of the polymer (Li et al., 2011).

Iron content of PAC-MNPs was quantified by iron assays (Gupta and Gupta, 2005). Briefly, 100 μl particle solution (1 mg/ml) was incubated with 100 μl of 50% hydrochloric acid solution at 50 °C for 2 h, followed by addition of 100 μl ammonium persulfate solution (1 mg/ml). After shaking for 15 min, 100 μl potassium thiocyanate solution (0.1 M) was added and incubated for another 15 min. The plate then read at 478 nm using UV–vis spectrophotometer (Infinite M200, Tecan, Durham, NC). In addition, the magnetic properties of PAC-MNPs were analyzed using vibrating sample magnetometer (VSM, KLA-Tencor EV7, San Jose, CA) and compared to those of bare MNPs. The samples consisting of equal amounts of iron oxide were embedded in wax and hysteresis loops were obtained by varying the magnetic fields at room temperature.

2.4. Drug loading and release

Dox was chosen as an anticancer drug model for encapsulating in PAC-MNPs. For drug loading, 12 mg PAC-MNPs and 2.5 mg Dox were suspended in 6 ml DI water and incubated at 4 °C for 3 days on a shaker to allow drug absorption in polymer shell. Dox-loaded PAC-MNPs were then collected by using a magnet and the supernatant containing un-loaded Dox was analyzed to quantify drug loading efficiency. Further, drug release was performed by incubating the drug-loaded nanoparticles (1 mg/ml) at 37 and 40 °C at pH 7.4 and pH of 6 and 7.4 at 37 °C to evaluate the effects of temperature and pH on the drug release independently. During 21 days of study, at each predetermined time point, the supernatants containing released drugs were collected by separating the nanoparticles using a magnet and the supernatant volumes were reconstituted with fresh DI water. The drug release samples were analyzed using a spectrophotometer at an excitation wavelength of 470 nm and emission wavelength of 585 nm.

2.5. *In vitro* cell studies

HDFs in DMEM, PZ-HPV-7 cells in Pr-EBM, and PC3 cells in RPMI were cultured in a humid environment at 37 °C with 5% CO_2 supply. DMEM and RPMI were supplemented with 10% serum and 1% penicillin–streptomycin, whereas PrEBM media was supplemented with PrEGM SingleQuots® Kit containing supplements and growth factors. All the primary cells up to passage 10 were used for the experiments. The cells were seeded in cell culture well plates and allowed to attach for 24 h prior to the experiments.

To evaluate the cytotoxicity of the nanoparticles on HDFs and PZ-HPV-7 cells, the cell culture media was replaced with the media containing PAC-MNPs or R11-PAC-MNPs at concentrations of 0–500 μg/ml. After 24 h of incubation, cell survival was evaluated using MTS assays following manufacturer's instructions (CellTiter 96® AQueous One Solution Cell Proliferation Assay, Promega, Madison, WI).

To evaluate the cellular uptake of the nanoparticles by PC3 and PZ-HPV-7 cells, the cell culture medium was replaced with the media containing PAC-MNPs or R11-PAC-MNPs at concentrations of 0–500 μg/ml. In another experiment, the effects of magnetic field on the cellular uptake were also evaluated by applying a magnetic field of 1.3 T using a magnet. After 6 h of incubation, the particle suspension was removed, and the cells were washed thoroughly with PBS and lysed using 1% Triton. The lysates were then analyzed for the iron content, as described above, and DNA content using Pico-Green DNA assays (Invitrogen Corp., Carlsbad, CA) per the manufacturer's instructions. The amount of iron was then normalized to the DNA content to determine the amount of particles internalized by the cells in the presence and the absence of magnetic field.

In order to determine the *in vitro* therapeutic efficacy of the nanoparticles, a pharmacokinetic study was conducted on PC3 cells. Four different groups, control (media only), free Dox, empty PAC-MNPs and Dox-loaded PAC-MNPs were used for this study. The cell culture medium was replaced with the media containing respective groups. The concentrations of free Dox and Dox-loaded PAC-MNPs used were determined based on the IC50 of Dox for PC3 cells (Tanaka et al., 2005). The cells were then incubated at 37 and 40°C to facilitate drug release from the Dox-loaded particles. Following 24 h of incubation, the cells were washed thrice with 1X PBS and the cell viability was assessed using MTS assays following manufacturer's instructions.

2.6. Statistical analysis

The results obtained were analyzed using one-way analysis of variance with $p < 0.05$ and post hoc comparisons (StatView, Version 5.0.1, SAS Institute Inc., Cary, NC). All the experiments were repeated multiple times with a sample size of four. All the results were presented as mean ± standard deviation.

3. Results and discussion

3.1. Synthesis and characterization of PAC nanoparticles and PAC-MNPs

The PAC nanoparticles were synthesized via graft copolymerization of monomers of NIPAAm, AAm, and chitosan in presence of TBHP as radical initiator and BIS as cross-

linking agent. The SEM (Fig. 1A) and TEM (Fig. 1B) images indicate that PAC nanoparticles are spherical in morphology and show a particle size of about 150 nm. FTIR spectra (Fig. 1C) show that NIPAAm, AAm and chitosan have been successfully polymerized since the C=O (1650 cm^{-1}) and N—H (1550 cm^{-1}) peaks of chitosan are intensified after the addition of NIPAAm and AAm as a result of a reaction between the functional groups present. Moreover, the inclusion of hydrophilic monomer AAm raised the LCST of PAC nanoparticles to 40°C as shown in Fig. 1D, whereas the LCST of PNIPAAm-chitosan nanoparticles was detected at 34 °C. Addition of AAm adds to the hydrophilic content of PNIPAAm and hence the LCST is increased. The temperature at which the transmittance of the nanoparticle solution reaches to 50%, is noted as the LCST (Li et al., 2011). Above its LCST, the hydrophobic interactions become dominant and the cloudiness of the solution is clearly visible, owing to the collapse of the polymer structure (Khodaverdi et al., 2012). The phase transition of PNIPAAm occurs due to the presence of hydrophilic amide groups and hydrophobic isopropyl groups in PNIPAAm (Siriwatwechakul et al., 2008).

Magnetic particles under the influence of an external alternating magnetic field undergo vibrations leading to heat generation (Kumar and Mohammad, 2011). Thus the application of external magnetic field to PAC-MNPs can be used for hyperthermia, and in the meantime, temperature responsive drug release from the particles as the temperature approaches 40 °C. Therefore, PAC was conjugated on the surface of MNPs. TEM image of bare MNPs (Fig. 2A) shows aggregation behavior of particles with the absence of a polymer coating. Whereas, TEM image of PAC-MNPs (Fig. 2B) shows well separated particles as well as a successful formation of core-shell structure and a particle size of around 150 nm. The black area represents the MNPs surrounded by a lighter grey polymeric shell of PAC. The DLS measurements at room temperature revealed a hydrodynamic diameter of 226 nm. Since the DLS measures the hydrodynamic diameter in water, there is a possibility of polymer swelling, leading to a higher size than observed by TEM (Dobrovolskaia et al., 2009). Iron assay results (as described earlier) suggested that the iron content of PAC-MNPs is 70% by weight. In the iron assay, Fe_3O_4 standards are considered to be 100% iron, and hence the iron content value obtained from these standards is normalized to 100%. Accordingly, the iron content of PAC-MNPs is determined to be 70% in correlation to the iron content value of the standard samples. VSM studies further validated that the PAC coating on MNPs does not affect their superparamagnetic properties as shown by the plot of magnetization in presence of applied field (Fig. 2C). The saturation magnetization values of bare MNPs and PAC-MNPs were about 70 and 68 emu/g, respectively. It has been shown that various polymer coatings affect the magnetic properties of MNPs (Sahoo et al., 2013). For example, poly(hydroxyethyl acrylate-b-*N*-iso-propylacrylamide), P(HEA-b-NIPAAm) grafted iron oxide nano-particles synthesized by Mu et al. (2011) showed a slight decrease in saturation magnetization, which the authors attributed to the grafting of PHEA and PNIPAAm to the iron oxide. Magnetic particles coated with PNIPAAm have been previously reported to retain their superparamagnetic properties (Lien and Wu, 2008). The slight decrease in the saturation magnetization value for PAC-MNPs may be attributed to the diamagnetic moment of the polymer coating on the MNPs. It is evident from the negligible hysteresis that our particles possess superparamagnetic properties which render them

suitable for applications in magnetic targeting (Yigit et al., 2012). Further, previous MRI studies done by our group on iron oxide containing polymeric nanoparticles have shown a distinct negative contrast with increasing concentration of the particles *in vitro* (Wadajkar et al., 2012b) and *in vivo* (Wadajkar et al., 2013). This indicates that particles containing iron oxide can be used for non-invasive imaging via MRI following administration.

Functionalization of MNPs helps prevent oxidation of the magnetic particles, reduces particle aggregation and increases particle stability since magnetic nanocarriers have been extensively investigated by many researchers for tumor applications (Lu et al., 2007). Recently, Jaiswal et al. (2012) synthesized and characterized PNIPAAm-chitosan-based magnetic nanogels for *in vivo* applications. Iron oxide nanoparticles in these nanogels were functionalized with citric acid or ethylenediamine or dimercaptosuccininc to provide stability to the gels. However, in our PAC-MNPs, we covalently functionalized MNPs with silane groups to facilitate stronger bonding of the polymer to the MNPs (Rahimi et al., 2009). In addition, silane functionalization provides increased biocompatibility and incorporation of a higher amount of MNPs into the polymercoating as compared to bare MNPs (Wadajkar et al., 2012a). The PAC coating on the MNPs provides a smart dual-responsive system for efficient drug delivery to the tumor with the added functionality of magnetic targeting. In addition to this magnetic targeting, the surface conjugation of R11 targeting molecules to PAC-MNPs as presented by this research project also ensures specific targeting of the particles to the prostate cancer, eliminating non-specific particle accumulation and toxicity.

3.2. Drug loading and release

The drug loading efficiency was calculated to be 86% which was comparable to loading efficiency values obtained in other studies on Dox-loaded PNIPAAm-based particles (Dai et al., 2010; Rahimi et al., 2010). Dual-responsive drug release from PAC-MNPs was evaluated and shown in Fig. 3. A significantly higher drug release was observed at the LCST of 40 °C (~80%) as compared to that at 37 °C (~33%) (Fig. 3A). This shows that the provision of external heat would result in enhanced drug release, thus increasing the therapeutic efficacy. Similar drug release profiles were observed by varying the acidity of the environment. Particles at pH of 6 showed a higher release rate (~55%) as compared to that at pH of 7.4 (~28%) at the end of 21 days (Fig. 3B). It can be concluded from these results that PAC-MNPs can be utilized as a temperature- and pH-triggered drug release system at the tumor site.

Due to the advantages of dual-responsive drug delivery systems, researchers have copolymerized thermo-responsive PNIPAAm with pH-responsive dimethylacrylamide (DMAAm), acrylic acid, or methacrylic acid (Cheng et al., 2013). The combination of high temperature and low pH has shown to be most effective in releasing the encapsulated drug to the tumor environment. For instance, Soppimath et al. (2005) showed that at 37 °C, particles with NIPAAm and DMAAm showed a higher release of Dox at pH of 6.6 compared to pH of 7.4. *In vitro* release profiles of Paclitaxel (PTX)-loaded diblock poly(*N*-isopropylacrylamide-co-acrylic acid)-polycaprolactone, nanoparticles also showed that the release was highest at acidic conditions (Zhang et al., 2007). In addition, higher drug release

was observed at the cancer acidic pH in studies conducted by other researchers on PNIPAAm-chitosan based particles (Li et al., 2009). Moreover, PNIPAAm-chitosan particles have also been used for thermo-responsive drug release. Hyperthermia treatment typically increases the temperature of the tumor site to up to 43 °C which triggers temperature responsive drug release from PAC-MNPs, ensuring higher release rate and cancer site-specific drug delivery.

3.3. *In vitro* cell studies

A major concern faced with the *in vivo* use of MNPs is their high cytotoxicity (Mahmoudi et al., 2011). Thus it is important to evaluate the cytotoxicity of our particles before investigating them for biological applications. The compatibility of PAC-MNPs and R11-PAC-MNPs were tested on HDFs and PZ-HPV-7 cells and the results showed viability of greater than 80% over 24 h, affirming their cytocompatible nature (Fig. 4A and B). PAC-MNPs exhibited excellent cytocompatibility up to a concentration of 500 μg/ml. Fan et al. (2008) have previously reported that PNIPAAm/chitosan nanoparticles were not harmful to human colon carcinoma cells and human dermal fibroblasts up to a concentration of 5 mg/ml. Further, the surface conjugation of R11 molecules on the PAC-MNPs did not alter the cell viability. Previously, it has been reported that the cell viability of fibroblasts after 24 h was around 74% with concentrations of iron oxide particles up to 500 μg/ml (Meenach et al., 2009). Further, poly(*N*-isopropylacrylamide-acrylamide-allyl-amine)-coated MNPs have been known to show cell viability of fibroblasts greater than 80% when incubated with particles for 24 h up to 500 μg/ml, whereas bare MNPs showed cell death of up to 62% for a concentration of 500 μg/ml (Rahimi et al., 2010). These results indicate that coating of MNPs with polymers would improve their cytocompatibility for future uses.

The presence of magnetic field and the targeting molecules conjugated on the particles further enhanced the uptake rate. Nanoparticle uptake by cells is an important parameter in estimating their efficacy, and cellular uptake of particles depends on a variety of factors including time, concentration, size, shape and surface chemistry of particles (Chithrani and Chan, 2007; Rahimi et al., 2010). An increasing trend in cellular uptake of PAC-MNPs by PC3 cells was observed with increasing concentration of particles up to 500 μg/ml, as shown in Fig. 5. The highest uptake was found in the group with the combination of R11-PAC-MNPs and magnetic field. However, there was no significant difference between the groups with and without R11. The cell-penetrating R11 peptides have been proven to have the ability to bind to prostate cells with high affinity (Zhou et al., 2012). Therefore, R11 peptides are incorporated in our nanoparticle design for achieving targeted delivery of particles to the prostate cancer *in vivo* in future. Though the specific nature of the peptides does aid in penetration of particles into the prostate cells, the effect is much higher in combination with the magnetic field. External magnetic field has been shown to enhance the cellular uptake of magnetic nanoparticles by the process of endocytosis. The attractive pull of the magnetic field on the magnetic particles aids in the particles penetrating the cell membrane. Rotation of MNPs and heat dissipation in presence of alternating magnetic field would further enhance the cell permeability (Min et al., 2010a). The strength and distance of the magnetic field from the cells have been considered to be significant factors in

determining the cellular uptake of MNPs in other studies (Min et al., 2013). As expected, the groups with an external magnetic showed better cellular uptake of PAC-MNPs.

Finally, the pharmacokinetic study results indicated that Dox-loaded PAC-MNPs caused higher cell death at 40 °C compared to the other treatment groups (Fig. 6). Assuming 100% cell viability in the untreated cells (control group) at 37 °C, the relative cell viability in the remaining groups was calculated. At 37 °C, about 74% and 81% of PC3 cells were viable when exposed to free Dox and Dox-loaded PAC-MNPs, respectively. However at 40 °C, only 54% and 42% of the cells exposed to free Dox and Dox-loaded PAC-MNPs, respectively, were viable indicating that the temperature-dependent Dox release from the PAC-MNPs was a major factor in causing cell death. These results support our previous findings where drug-loaded core-shell thermo-responsive nanoparticles caused higher cell death in B16F10 melanoma cells at 41 °C than at 37 °C (Wadajkar et al., 2012a). Similarly, Dox-loaded thermally crosslinked superparamagnetic iron oxide-aptamer bioconju-gates prepared by Wang et al. (2008) also showed similar potency as free Dox *in vitro* when incubated with PC3 cells. Heat might also be another factor in causing cell death by hyperthermia in our study, which is evident by the ~87% cell viability in the control group at 40 °C as opposed to 100% cell viability in the control group at 37 °C.

4. Conclusions

A copolymer of temperature-responsive PNIPAAm-AAm and chitosan has been coated on MNPs to devise a nanoparticulate drug delivery system for cancer treatment. The presence of chitosan improves our previously described nanoparticles with increased degradability and pH responsiveness. In the given study, PAC-MNPs were synthesized and characterized, possessing super-paramagnetic properties and dual-responsiveness as well as high cytocompatibility. The LCST of PAC was increased by incorporating AAm monomers. Improved drug release profiles were observed at the LCST of PAC-MNPs (40 °C) and also at pH 6. R11-conjugated PAC-MNPs further demonstrate high cytocompatibility and cellular uptake and aid in targeted release of drugs at the tumor site. Dox-loaded PAC MNPs also showed good therapeutic efficacy *in vitro* by significantly reducing the PC3 cell viability at 40 °C compared to body temperature, thus demonstrating their temperature-dependent release kinetics. To develop PAC-MNPs as a platform technology for cancer targeting, imaging, and therapy, our future studies are aimed at evaluating the *in vivo* pharmacokinetics and *in vivo* efficacies of the PAC-MNPs in animal cancer models.

Acknowledgments

We would like to acknowledge the financial support from the U.S. Department of Defense, DOD W81XWH-09-1-0313. We also thank Ms. Alicia J. Sisemore for her help with the manuscript editing. The content is solely the responsibility of the authors and does not necessarily represent the official views of the DOD.

References

Cheng R, Meng F, Deng C, Klok HA, Zhong Z. Dual and multi-stimuli responsive polymeric nanoparticles for programmed site-specific drug delivery. Biomaterials. 2013; 34:3647–3657. [PubMed: 23415642]

Chithrani BD, Chan WCW. Elucidating the mechanism of cellular uptake and removal of protein-coated gold nanoparticles of different sizes and shapes. Nano Letters. 2007; 7:1542–1550. [PubMed: 17465586]

Chuang CY, Don TM, Chiu WY. Synthesis of chitosan-based thermo-and pH-responsive porous nanoparticles by temperature-dependent self-assembly method and their application in drug release. Journal of Polymer Science Part A: Polymer Chemistry. 2009; 47:5126–5136.

Chuang CY, Don TM, Chiu WY. Synthesis and characterization of stimuli-responsive porous/hollow nanoparticles by self-assembly of chitosan-based graft copolymers and application in drug release. Journal of Polymer Science Part A: Polymer Chemistry. 2010; 48:2377–2387.

Cui Z, Lee BH, Pauken C, Vernon BL. Degradation, cytotoxicity, and biocompatibility of NIPAAm-based thermosensitive, injectable, and biore-sorbable polymer hydrogels. Journal of Biomedical Materials Research. 2011; 98:159–166. [PubMed: 21548065]

Curcio M, Gianfranco Spizzirri U, Iemma F, Puoci F, Cirillo G, Parisi OI, Picci N. Grafted thermo-responsive gelatin microspheres as delivery systems in triggered drug release. European Journal of Pharmaceutics and Biopharma-ceutics. 2010; 76:48–55.

Dai W, Zhang Y, Du Z, Ru M, Lang M. The pH-induced thermosensitive poly (NIPAAm-co-AAc-co-HEMA)-g-PCL micelles used as a drug carrier. Journal of Materials Science. 2010; 21:1881–1890. [PubMed: 20217189]

Danhier F, Feron O, Preat V. To exploit the tumor microenvironment: passive and active tumor targeting of nanocarriers for anti-cancer drug delivery. Journal of Controlled Release. 2010; 148:135–146. [PubMed: 20797419]

Dash M, Chiellini F, Ottenbrite RM, Chiellini E. Chitosan-A versatile semi-synthetic polymer in biomedical applications. Progress in Polymer Science. 2011; 36:981–1014.

Dobrovolskaia MA, Patri AK, Zheng J, Clogston JD, Ayub N, Aggarwal P, Neun BW, Hall JB, McNeil SE. Interaction of colloidal gold nanoparticles with human blood: effects on particle size and analysis of plasma protein binding profiles. Nanomedicine. 2009; 5:106–117. [PubMed: 19071065]

Fan L, Wu H, Zhang H, Li F, Yang T-h, Gu C-h, Yang Q. Novel super pH-sensitive nanoparticles responsive to tumor extracellular pH. Carbohydrate Polymers. 2008; 73:390–400.

Fitzpatrick SD, Jafar Mazumder MA, Lasowski F, Fitzpatrick LE, Sheardown H. PNIPAAm-grafted-collagen as an injectable, in situ gelling, bioactive cell delivery scaffold. Biomacromolecules. 2010; 11:2261–2267. [PubMed: 20695495]

Gupta AK, Gupta M. Cytotoxicity suppression and cellular uptake enhancement of surface modified magnetic nanoparticles. Biomaterials. 2005; 26:1565–1573. [PubMed: 15522758]

Jaiswal M, Mehta S, Banerjee R, Bahadur D. A comparative study on thermoresponsive magnetic nanohydrogels: role of surface-engineered magnetic nanoparticles. Colloid & Polymer Science. 2012; 290:607–617.

Khodaverdi E, Rajabi O, Farhadi F, Jalali A, Tekie FSM. Preparation and investigation of poly (*N*-isopropylacrylamide-acrylamide) membranes in temperature responsive drug delivery. Iranian Journal of Basic Medical Sciences. 2012; 13:102–110.

Kumar CS, Mohammad F. Magnetic nanomaterials for hyperthermia-based therapy and controlled drug delivery. Advanced Drug Delivery Reviews. 2011; 63:789–808. [PubMed: 21447363]

Li F, Wu H, Zhang H, Li F, Gu C-h, Yang Q. Antitumor drug Paclitaxel-loaded pH-sensitive nanoparticles targeting tumor extracellular pH. Carbohydrate Polymers. 2009; 77:773–778.

Li G, Guo L, Meng Y, Zhang T. Self-assembled nanoparticles from thermo-sensitive polyion complex micelles for controlled drug release. Chemical Engineering Journal. 2011; 174:199–205.

Lien YH, Wu TM. Preparation and characterization of thermosensitive polymers grafted onto silica-coated iron oxide nanoparticles. Journal of Colloid and Interface Science. 2008; 326:517–521. [PubMed: 18667211]

Lu AH, Salabas EL, Schüth F. Magnetic nanoparticles: synthesis, protection, functionalization, and application. Angewandte Chemie International Edition. 2007; 46:1222–1244.

Mahmoudi M, Laurent S, Shokrgozar MA, Hosseinkhani M. Toxicity evaluations of superparamagnetic iron oxide nanoparticles: cell “vision” versus physicochemical properties of nanoparticles. ACS Nano. 2011; 5:7263–7276. [PubMed: 21838310]

Meenach SA, Anderson AA, Suthar M, Anderson KW, Hilt JZ. Biocompatibility analysis of magnetic hydrogel nanocomposites based on poly(*N*-isopropylacrylamide) and iron oxide. Journal of Biomedical Materials Research. 2009; 91:903–909. [PubMed: 19090484]

Min KA, Yu F, Yang VC, Zhang X, Rosania GR. Transcellular transport of heparin-coated magnetic iron oxide nanoparticles (Hep-MION) under the influence of an applied magnetic field. Pharmaceutics. 2010a; 2:119–135. [PubMed: 21152371]

Min KH, Kim JH, Bae SM, Shin H, Kim MS, Park S, Lee H, Park RW, Kim IS, Kim K, Kwon IC, Jeong SY, Lee DS. Tumoral acidic pH-responsive MPEG-poly(beta-amino ester) polymeric micelles for cancer targeting therapy. Journal of Controlled Release. 2010b; 144:259–266. [PubMed: 20188131]

Min KA, Shin MC, Yu F, Yang M, David AE, Yang VC, Rosania GR. Pulsed magnetic field improves the transport of iron oxide nanoparticles through cell barriers. ACS Nano. 2013

Mu B, Wang T, Wu Z, Shi H, Xue D, Liu P. Fabrication of functional block copolymer grafted superparamagnetic nanoparticles for targeted and controlled drug delivery. Colloids and Surfaces A: Physicochemical and Engineering Aspects. 2011; 375:163–168.

Patenaude M, Hoare T. Injectable, degradable thermoresponsive poly (*N*-isopropylacrylamide) hydrogels. ACS Macro Letters. 2012; 1:409–413.

Rahimi M, Yousef M, Cheng Y, Meletis EI, Eberhart RC, Nguyen K. Formulation and characterization of a covalently coated magnetic nanogel. Journal of Nanoscience and Nanotechnology. 2009; 9:4128–4134. [PubMed: 19916419]

Rahimi M, Wadajkar A, Subramanian K, Yousef M, Cui W, Hsieh JT, Nguyen KT. In vitro evaluation of novel polymer-coated magnetic nanoparticles for controlled drug delivery. Nanomedicine. 2010; 6:672–680. [PubMed: 20172050]

Rosen JE, Chan L, Shieh DB, Gu FX. Iron oxide nanoparticles for targeted cancer imaging and diagnostics. Nanomedicine: Nanotechnology, Biology and Medicine. 2012; 8:275–290.

Sahoo B, Devi KS, Banerjee R, Maiti TK, Pramanik P, Dhara D. Thermal and pH responsive polymer-tethered multifunctional magnetic nanoparticles for targeted delivery of anticancer drug. ACS Applied Materials and Interfaces. 2013

Schmaljohann D. Thermo- and pH-responsive polymers in drug delivery. Advanced Drug Delivery Reviews. 2006; 58:1655–1670. [PubMed: 17125884]

Sethuraman VA, Bae YH. TAT peptide-based micelle system for potential active targeting of anti-cancer agents to acidic solid tumors. Journal of Controlled Release. 2007; 118:216–224. [PubMed: 17239466]

Siriwatwechakul W, Teraphongphom N, Ngaotheppitak V, Kunataned S. Thermo-sensitive hydrogel: control of hydrophilic-hydrophobic transition. International Journal of Chemical & Biomolecular Engineering. 2008; 1:165–170.

Soppimath KS, Tan DCW, Yang YY. pH-Triggeredthermallyresponsivepolymer core–shell nanoparticles for drug delivery. Advanced Materials. 2005; 17:318–323.

Sun C, Lee JSH, Zhang M. Magnetic nanoparticles in MR imaging and drug delivery. Advanced Drug Delivery Reviews. 2008; 60:1252–1265. [PubMed: 18558452]

Tanaka M, Rosser CJ, Grossman HB. PTEN gene therapy induces growth inhibition and increases efficacy of chemotherapy in prostate cancer. Cancer Detection and Prevention. 2005; 29:170–174. [PubMed: 15829377]

Wadajkar AS, Bhavsar Z, Ko CY, Koppolu B, Cui W, Tang L, Nguyen KT. Multifunctional particles for melanoma-targeted drug delivery. Acta Biomater-ialia. 2012a; 8:2996–3004.

Wadajkar AS, Kadapure T, Zhang Y, Cui W, Nguyen KT, Yang J. Dual-imaging enabled cancer-targeting nanoparticles. Advanced Healthcare Materials. 2012b; 1:450–456. [PubMed: 23061030]

Wadajkar AS, Menon JU, Tsai YS, Gore C, Dobin T, Gandee L, Kangasniemi K, Takahashi M, Manandhar B, Ahn JM, Hsieh JT, Nguyen KT. Prostate cancer-specific thermo-responsive polymer-coated iron oxide nanoparticles. Biomaterials. 2013; 34:3618–3625. [PubMed: 23419645]

Wang AZ, Bagalkot V, Vasilliou CC, Gu F, Alexis F, Zhang L, Shaikh M, Yuet K, Cima MJ, Langer R, Kantoff PW, Bander NH, Jon S, Farokhzad OC. Superparamagnetic iron oxide nanoparticle-

aptamer bioconjugates for combined prostate cancer imaging and therapy. ChemMedChem. 2008; 3:1311–1315. [PubMed: 18613203]

Yigit MV, Moore A, Medarova Z. Magnetic nanoparticles for cancer diagnosis and therapy. Pharmaceutical Research. 2012; 29:1180–1188. [PubMed: 22274558]

Yomota C, Komuro T, Kimura T. Studies on the degradation of chitosan films by lysozyme and release of loaded chemicals. Yakugaku Zasshi. 1990; 110:442–448. [PubMed: 2213531]

Zhang L, Guo R, Yang M, Jiang X, Liu B. Thermo and pH dual-responsive nanoparticles for anti-cancer drug delivery. Advanced Materials. 2007; 19:2988–2992.

Zhou J, Liu W, Pong RC, Hao G, Sun X, Hsieh JT. Analysis of oligo-arginine cell-permeable peptides uptake by prostate cells. Amino Acids. 2012; 42:1253–1260. [PubMed: 21120551]

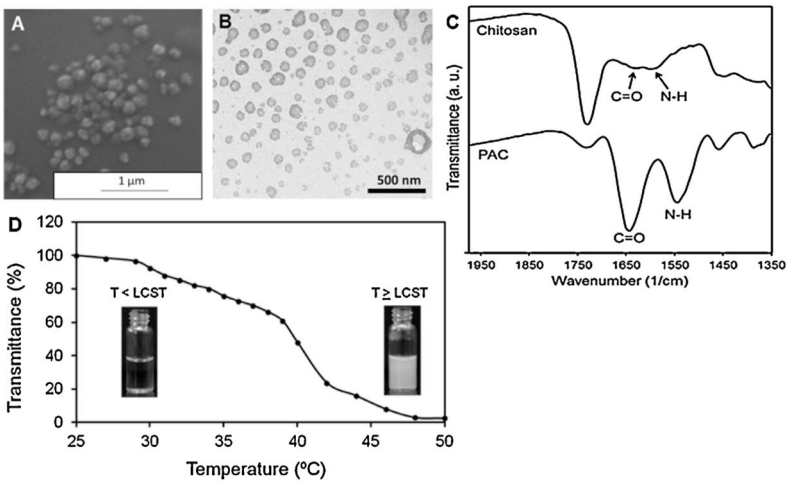

Fig. 1.

Characterization of PAC nanoparticles. (A) SEM image of PAC nanoparticles (avg. diameter: 150 nm). (B) TEM image of PAC nanoparticles demonstrating relatively spherical morphology. (C) FTIR of Chitosan and PAC nanoparticles showing presence of all the significant chemical bonds. (D) LCST of PAC nanoparticles at 40 °C when transmittance decreased to 50%.

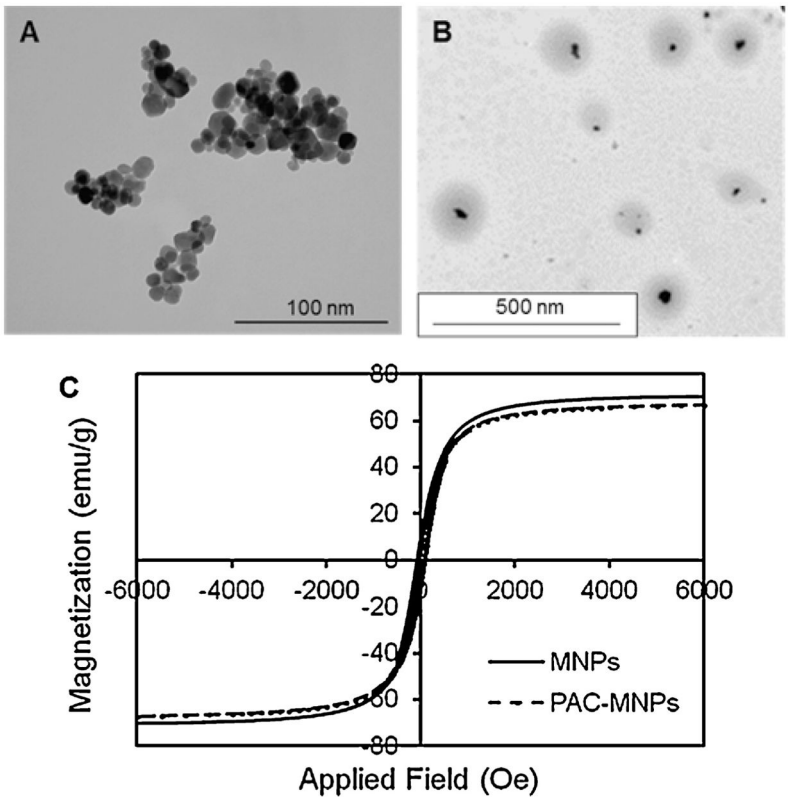

Fig. 2.

Characterization of PAC-MNPs. (A) TEM image of MNPs (avg. diameter: 10 nm) (B) TEM image of PAC-MNPs (avg. diameter: 150 nm) showing core-shell structure. (C) Magnetic hysteresis loops of bare MNPs and PAC-MNPs exhibiting superparamagnetic behaviors.

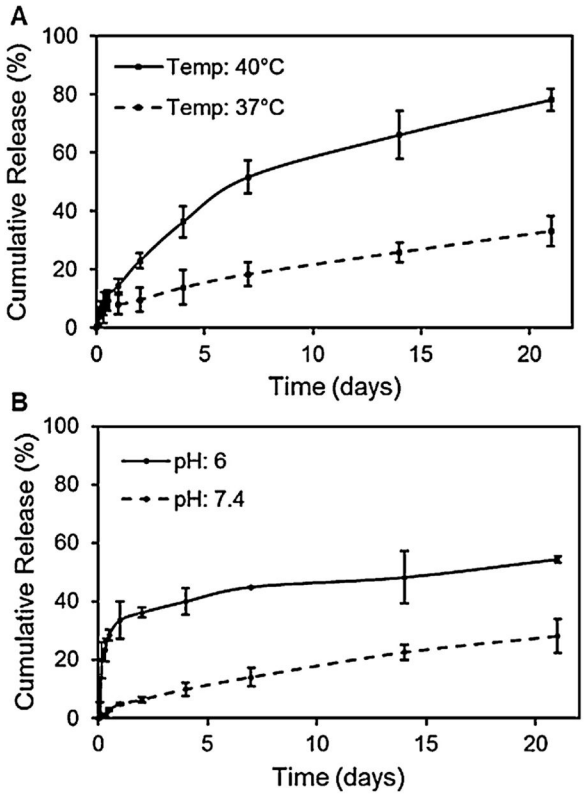

Fig. 3.

Dual-responsive (temperature and pH) Dox release profiles from PAC-MNPs showing (A) higher release of Dox at 40 °C (~78%) as compared to 37 °C (~33%) and (B) higher release at pH of 6 (~55%) as compared to pH of 7.4 (~28%) after 21 days.

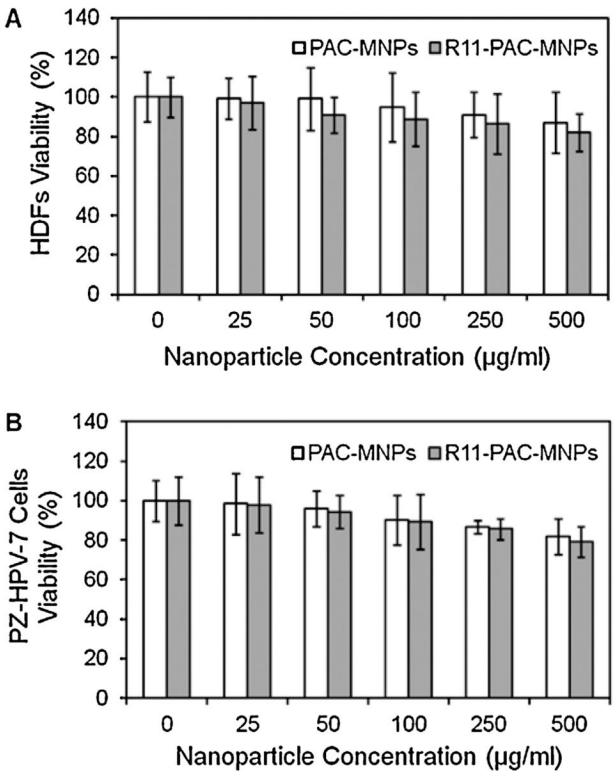

Fig. 4.

Cytotoxicity of nanoparticles on (A) HDFs and (B) PZ-HPV-7 cells after 24 h of nanoparticle incubation showing more than 80% cell viability up to 500 µg/ml concentration.

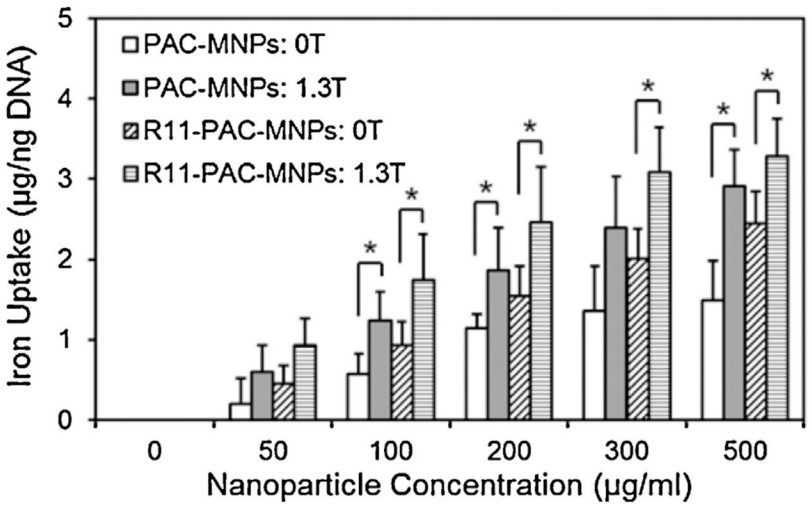

Fig. 5.

Cellular uptake of nanoparticles by PC3 cells after 24 h of nanoparticle incubation in the absence and presence of a magnetic field (1.3 T), showing higher uptake of particles in presence of magnetic field and R11 peptides (*p <0.05).

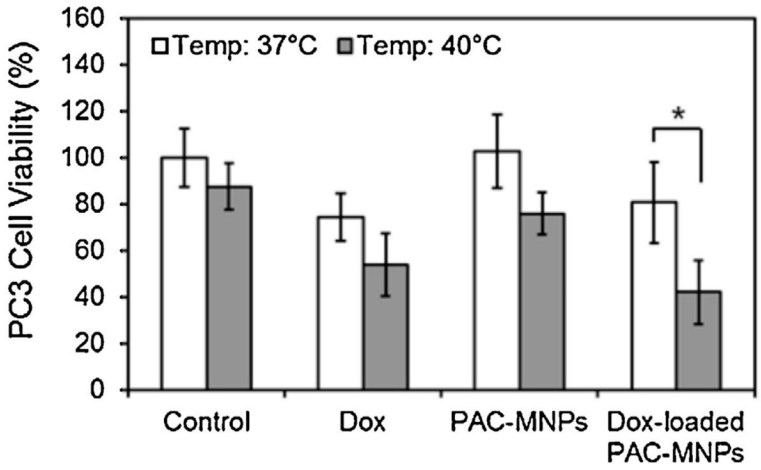

Fig. 6.

Effects of free Dox, empty PAC-MNPs, and Dox-loaded PAC-MNPs on PC3 cell survival at 37 °C and 40 °C, showing significant cell mortality in case of Dox-loaded PAC-MNPs at 40 °C compared to at 37 °C (*p <0.05).